Role of interparticle friction and particle-scale elasticity in the shear-strength mechanism of three-dimensional granular media

S. J. Antony[1,*] and N. P. Kruyt[2,†]
[1]*Institute of Particle Science and Engineering, University of Leeds, Leeds LS2 9JT, United Kingdom*
[2]*Department of Mechanical Engineering, University of Twente, P. O. Box 217, 7500 AE Enschede, The Netherlands*
(Received 20 November 2008; published 30 March 2009)

The interlink between particle-scale properties and macroscopic behavior of three-dimensional granular media subjected to mechanical loading is studied intensively by scientists and engineers, but not yet well understood. Here we study the role of key particle-scale properties, such as interparticle friction and particle elastic modulus, in the functioning of dual contact force networks, viz., strong and weak contacts, in mobilizing shear strength in dense granular media subjected to quasistatic shearing. The study is based on three-dimensional discrete element method in which particle-scale constitutive relations are based on well-established nonlinear theories of contact mechanics. The underlying distinctive contributions of these force networks to the macroscopic stress tensor of sheared granular media are examined here in detail to find out how particle-scale friction and particle-scale elasticity (or particle-scale stiffness) affect the mechanism of mobilization of macroscopic shear strength and other related properties. We reveal that interparticle friction mobilizes shear strength through bimodal contribution, i.e., through both major and minor principal stresses. However, against expectation, the contribution of particle-scale elasticity is mostly unimodal, i.e., through the minor principal stress component, but hardly by the major principal stress. The packing fraction and the geometric stability of the assemblies (expressed by the mechanical coordination number) increase for decrease in interparticle friction and elasticity of particles. Although peak shear strength increases with interparticle friction, the deviator strain level at which granular systems attain peak shear strength is mostly independent of interparticle friction. Granular assemblies attain peak shear strength (and maximum fabric anisotropy of strong contacts) when a critical value of the mechanical coordination number is attained. Irrespective of the interparticle friction and elasticity of the particles, the packing fraction and volumetric strain are constant during steady state. Volumetric strain in sheared granular media increases with interparticle friction and elasticity of the particles. We show that the elasticity of the particles does not enhance dilation in frictionless granular media. The results presented here provide additional understanding of the role of particle-scale properties on the collective behavior of three-dimensional granular media subjected to shearing.

DOI: 10.1103/PhysRevE.79.031308 PACS number(s): 81.05.Rm

I. INTRODUCTION

Realistic description of the constitutive behaviour of granular materials is desired in many fundamental as well as applied research fields. However, the mechanical behavior of granular materials is extremely complex when viewed at the microscale and below. They often display surprising behaviors under mechanical loading [1–5]. Significant numbers of studies report some advancement on how stress transmission occurs in granular media under a given boundary loading condition (e.g., [1–10]). It is now recognized that granular assemblies, even when subjected to uniform loading, display nonhomogeneous force transmission characteristics at particle contacts. The forces are transmitted by relatively chain-like sparse networks (commonly referred to as "force chains") of heavily loaded contacts [1–4,7–9]. More recently, studies have shown that the networks of contacts carrying forces can be grouped into two subnetworks, viz., strong and weak force networks. The strong contacts carry forces larger than the average normal force in the assembly ($f>1$, $f=N/\langle N\rangle$, N is the normal force and $\langle N\rangle$ is its average over all contacts) whereas the weak contacts carry less than average force [2,4,9,10]. Interestingly, the strong and weak contacts play distinctive roles in sheared granular media. For granular media subjected to quasi-static shearing, the strong contacts form a solidlike backbone for transmitting forces, whereas the weak contacts provide stability against buckling to the strong force chains. The nature of stress experienced by these weak contacts is mostly hydrostatic (liquidlike) and sliding occurs more dominantly among the weak contacts [9–13].

Studies on the microscopic origin of shear strength in three-dimensional granular media [12,13] have shown a strong correlation between shear strength and directional anisotropy in the alignment of strong contacts. It is pointed out that shear strength of granular media depends on their ability to develop highly anisotropic strong contacts. The ability of granular media to develop strong contacts is influenced by particle-scale properties and packing conditions [13]. Similar to force chains, other studies [2] have also identified mobile networks of contacts (in which relative displacement is dominant) and work networks (in which work spent is dominant) during shearing. They also suggested possible correlations between the work network and the force-displacement networks [2].

Analysis of granular systems using advanced modeling tools, such as the discrete element method (DEM) [14], pro-

*S.J.Antony@leeds.ac.uk
†n.p.kruyt@utwente.nl

vides the ability to study the influence of particle-scale properties on micromechanical and nanomechanical characteristics of particulate assemblies under a range of mechanical loading conditions [2–5,10,15].

Using DEM, recent studies have shown that the shear strength of granular systems is primarily due to the normal forces at particle contacts and that the contribution of tangential contact forces is smaller [9–13]. However, it is not yet well known as to how friction and elasticity at the particle scale influence the individual stress contributions of normal and tangential forces carried by the strong and weak contacts and their subsequent effects on the mechanism of mobilizing shear strength in three-dimensional granular systems—this aspect is addressed in the present work in a systematic manner.

II. SIMULATIONS

The DEM simulation methodology used here is identical to the one implemented for studying force-transmission properties in elastic and frictional static granular packing [16]. The spherical particles considered here are cohesionless, but elastic and frictional. The interparticle interactions are based on well-known theories of contact mechanics. The normal and tangential force-displacement relations are governed by the Hertzian [17] and Mindlin-Deresiewicz [18] laws, respectively.

For the purpose of analysis, the evolution of stress tensor, fabric tensor, contacts, packing density, and volumetric strain are computed in sheared granular assemblies [2,14]. The average stress tensor σ_{ij} in a granular assembly can be directly computed as a sum of dyadic products associated with its M contacts [14]:

$$\sigma_{ij} = \frac{1}{V} \sum_{xy \in M} l_i^{xy} f_j^{xy} \tag{1}$$

where V is the assembly volume. Each product is for a contact xy between particles x and y, and the pair xy is an element in the set M of all contacts. The branch vector $\boldsymbol{l}^{xy}$ connects the center of mass of a particle x to the center of mass of particle y; and $\boldsymbol{f}^{xy}$ is the contact force exerted by particle x on y. By decomposing the contact force vectors into normal and tangential components $\boldsymbol{f}^{xy}=f^{xy,n}\boldsymbol{n}^{xy}+f^{xy,t}\boldsymbol{t}^{xy}$, with $\boldsymbol{l}^{xy}=l^{xy}\boldsymbol{n}^{xy}$ for spherical particles (l^{xy} is the length of the branch vector $\boldsymbol{l}^{xy}$), σ_{ij} can be written as [2,14,19]

$$\sigma_{ij} = \frac{1}{V} \sum_{xy \in M} l^{xy}[f^{xy,n}(n_i^{xy} n_j^{xy}) + f^{xy,t}(n_i^{xy} t_j^{xy})], \tag{2}$$

where $\boldsymbol{n}^{xy}$ is the outward unit normal of particle x at contact xy, and $\boldsymbol{t}^{xy}$ is the unit tangential vector aligned with the tangential component of contact force.

There are different ways by which the anisotropy of the contact orientation distribution can be represented. Here, the distribution of contact orientations is characterized by the widely used "fabric tensor" ϕ_{ij}, suggested by Satake [20], as

$$\phi_{ij} = (1/M) \sum_{xy \in M}^{M} n_i^{xy} n_j^{xy}. \tag{3}$$

Analogously, $\phi_{ij,s}$ denotes the fabric anisotropy of strong contacts [10,13,19].

The simulation assembly consists of 8000 polydispersed spheres following an approximately normal distribution with mean size 100 μm (ten different sizes of the spheres were used in the diameter range 100 ± 5 μm). We considered two cases of elastic modulus (E) of particles, viz., 70 GPa, hard ($E/p=700\,000$, where p is the constant mean stress of the assembly) and 70 MPa, soft ($E/p=700$). All the particles were assigned with Poisson's ratio equal to 0.5. Three cases of interparticle friction between particles were considered, viz., $\mu=0.1$, 0.25, and 0.5. The particles were initially randomly generated within a cuboidal periodic cell with zero contacts. The particles were then subjected to isotropic compression under strain rate of 1×10^{-5} s^{-1} in a large number of small time steps. During isotropic compression, a servo-control mechanism [10] was periodically introduced to attain desired mean stress level and the samples were equilibrated to attain constant values of coordination number and packing density. These measures minimized the transient inertial effects that could have otherwise biased the presumed quasi-static condition. More details of the sample preparation procedure can be found in Ref. [10]. The initial assemblies thus created were in dense packing (the initial packing density of the hard and soft samples was 0.635 and 0.690, respectively). The initial contact indentations were less than 0.04% of the mean particle size. All the initial assemblies were isotropic and homogeneous and held under a mean stress of 100 kPa. The assemblies were then slowly sheared by applying axisymmetric triaxial compression loading under constant mean stress condition [Fig. 1(a), $\sigma_{11} > \sigma_{22}=\sigma_{33}$, $p=100$ kPa] in a periodic cell to eliminate wall effects.

III. RESULTS

For the purpose of analysis, the normal and tangential stress contributions of strong and weak contacts, to the major principal stress component σ_{11} and the minor principal stress component σ_{33} are extracted from (particle-scale information of) the simulation results [Eq. (2)] and presented in Figs. 1–6. In these plots, unless mentioned otherwise, the symbol $>$ corresponds to the contribution of strong contacts, whereas the $<$ symbol corresponds to the contribution of weak contacts. N and T correspond to the normal and tangential stress contributions, respectively. In the notation for the stress tensor, the first symbol of the superscript represents the normal or tangential stress contribution to the stress tensor and the second symbol represents which network of contacts made that contribution (i.e., whether contributed by strong or weak contacts). For example, the normal stress contribution of strong contacts to the major principal stress σ_{11} is denoted as $\sigma_{11}^{N>}$. The macroscopic shear strength is presented in terms of (shear) stress ratio=deviator stress (q)/mean stress (p), $q=\sigma_{11}-\sigma_{33}$, $p=\sigma_{kk}/3$, and deviator strain=$\varepsilon_{11}-\varepsilon_{33}$, where ε_{ij} is the strain tensor. Furthermore

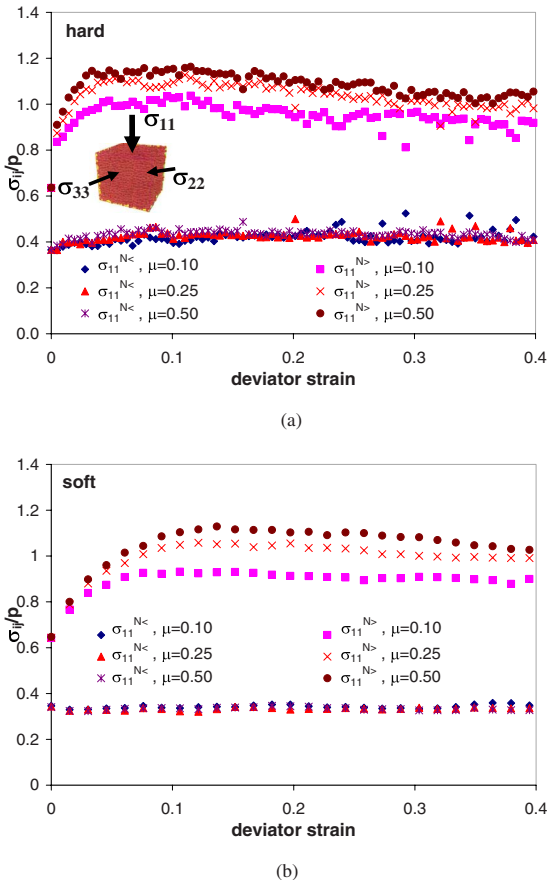

(a)

(b)

FIG. 1. (Color online) Variation of the normal stress contribution of strong and weak contacts to σ_{11} in hard (a) and soft (b) sheared granular assemblies.

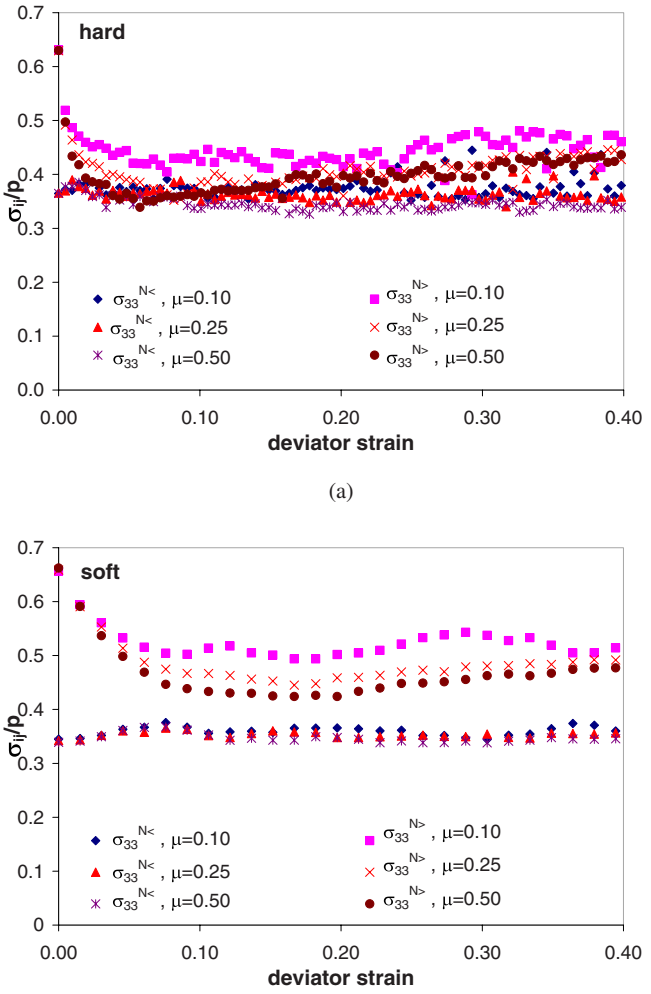

(a)

(b)

FIG. 2. (Color online) Variation of the normal stress contribution of strong and weak contacts to σ_{33} in hard (a) and soft (b) sheared granular assemblies.

$$\sigma_{ij}^{N} = \sigma_{ij}^{N>} + \sigma_{ij}^{N<}. \tag{4}$$

Similar equations can be written for the tangential stress contribution of the principal stress and the overall principal stresses as summation of total normal and tangential stress contributions of both the strong and weak contacts.

A. Role analysis of interparticle friction and elasticity of particles

In all the plots presented in this section (Figs. 1–6), the stresses σ_{ij} that contribute to the shear stress ratio are normalized by the mean stress of the assembly for both the hard and soft systems and plotted as dimensionless numbers in the vertical axis of each plot. The deviator strain is plotted in the horizontal axis.

1. Normal and tangential stress contributions of strong and weak contacts to principal stress components

The normal and tangential stress contributions of the strong and weak contacts to the major (σ_{11}) and minor (σ_{33}) principal stress components are presented in Figs. 1 and 2, respectively, for both the hard and soft systems subjected to shearing. It is evident that, irrespective of elasticity of particles, increase in interparticle friction enhances the normal stress contribution of strong contacts to the major principal stress, but decreases this contribution to the minor principal stress during shearing. At the same time, the normal stress contribution of weak contacts to both the major and minor principal stress is independent of interparticle friction. Furthermore, the magnitude of this measure remains practically constant throughout shearing. Figure 3 shows the tangential stress contribution of strong and weak contacts to the major principal stress for both the hard and soft assemblies. In agreement with previous studies [10–13], overall, the magnitude of this measure is less than about 10% of the normal stress contribution of strong contacts to the major principal stress (Figs. 1 and 3). Though not presented here, we have also verified that the tangential stress contribution of strong and weak contacts to minor principal stress is always small (less than about 4%) and decreased with increased interparticle friction. However, we observe (Fig. 3) that interparticle friction enhances (close to proportionally to μ) the tangential stress contribution of both strong and weak contacts to major principal stress. For the purposes of analysis, the above conclusions are summarized in Table I. As a result of the above-mentioned effects, an increase in interparticle friction en-

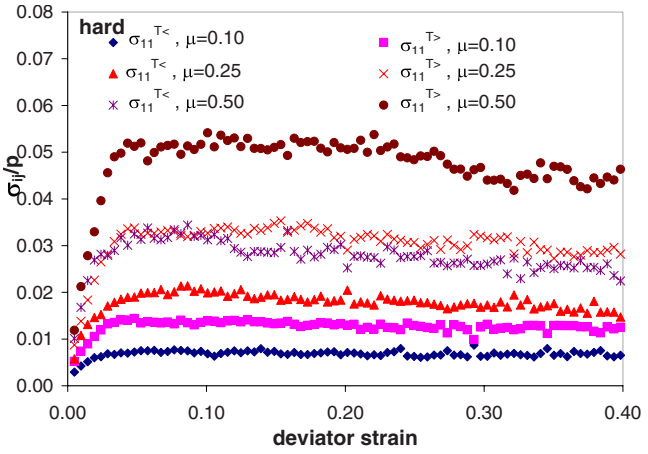

(a)

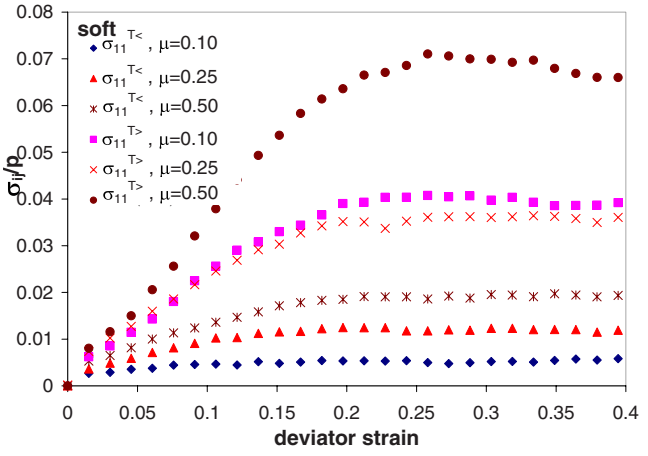

(b)

FIG. 3. (Color online) Variation of the tangential stress contribution of strong and weak contacts to σ_{11} in hard (a) and soft (b) sheared granular assemblies.

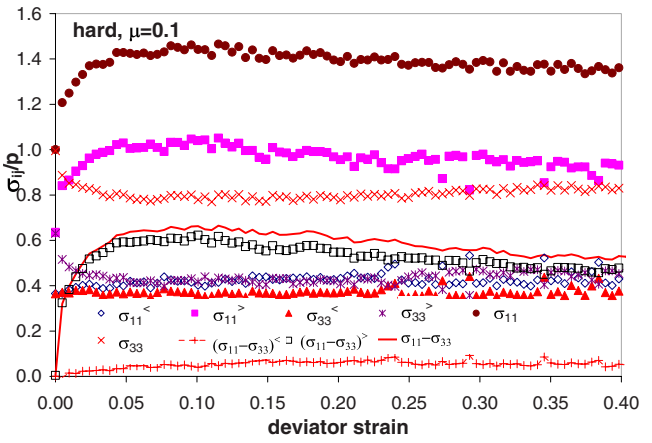

(a)

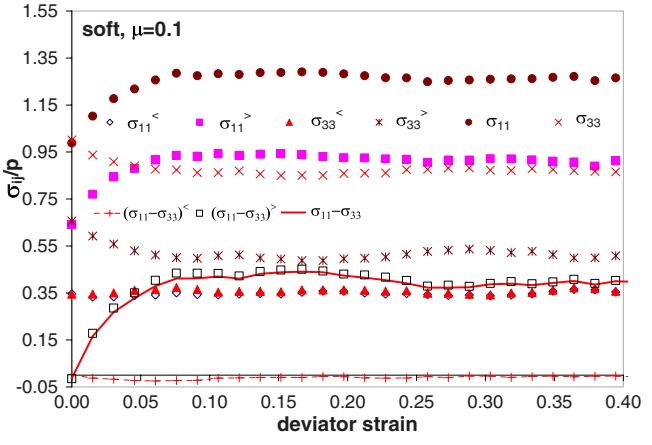

(b)

FIG. 4. (Color online) Contribution of strong and weak contacts to principal stresses and deviator stress (μ=0.1) in hard (a) and soft (b) granular assemblies under shearing.

hances the major principal stress, while decreasing the minor principal stress. Thus, through the *dual mode* actions of major and minor principal stresses, interparticle friction enhances the shear strength (which is proportional to the deviator stress component) of granular media.

Now we focus our attention on the effects of elasticity of the particles (or particle stiffness) in the above-presented results (Figs. 1–3). We find that (i) elasticity of particles enhances the normal stress contribution of the strong contacts to major principal stress only before the system attains peak shear strength (prepeak regime). During the postpeak period, for a given value of interparticle friction, the elasticity of the particles does not influence the normal stress contribution of strong contacts to σ_{11} (Fig. 1) (ii) For a given value of interparticle friction, the normal stress contribution of the strong contacts to σ_{33} in the soft system is always higher than that of the hard system during shearing (Fig. 2)—i.e., $\sigma_{33}^{N>}$ decreases with increase of elasticity of particles. (iii) The normal stress contribution of weak contacts to σ_{11} marginally increases with elasticity of particles, but its contribution to σ_{33} is independent of elasticity of particles (and interparticle friction) (Fig. 2). (iv) Increase in elasticity of particles decreases the tangential stress contribution of both strong and weak contacts to σ_{11} (Fig. 3) and σ_{33} (though not presented here). These conclusions are summarized in Table I.

2. *Analysis of the contribution of strong and weak contacts to principal and deviator stress*

To get further insights on the combined effects of interparticle friction and elasticity, for each case of interparticle friction, we present the combined contribution of normal and tangential contact forces of strong and weak contacts to the (i) individual principal stress components of strong and weak contacts (ii) deviator stress component of strong and weak contacts, and (iii) total deviator stress component for both hard and soft systems in Figs. 4–6. From these figures, we verified that the strong contacts dominantly contribute to the deviator stress of the assemblies, in agreement with other studies [2,13]. The deviator stress component of weak contacts is practically negligible. We observe that, in hard systems, the contribution of weak contacts to both the major and minor principal stresses is fairly independent of interparticle friction at all stages of shearing (i.e., $\sigma_{11}^{<}=\sigma_{33}^{<}$ throughout

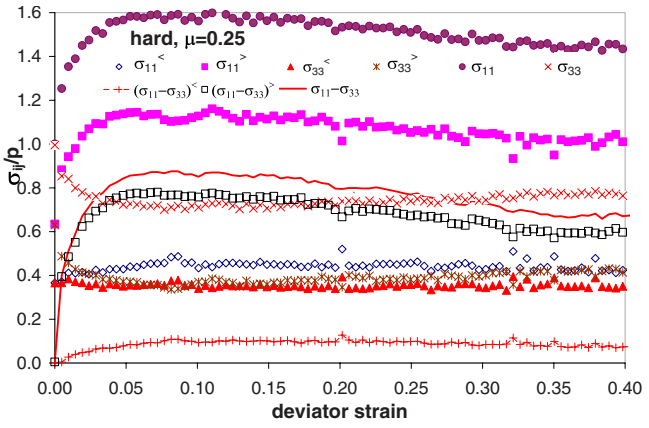

(a)

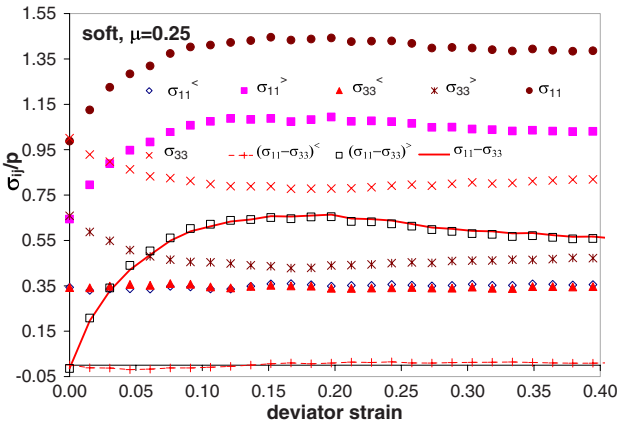

(b)

FIG. 5. (Color online) Contribution of strong and weak contacts to principal stresses and deviator stress (μ=0.25) in hard (a) and soft (b) granular assemblies under shearing.

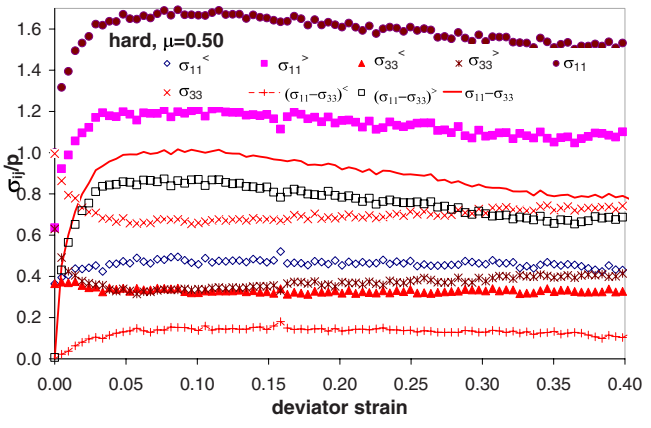

(a)

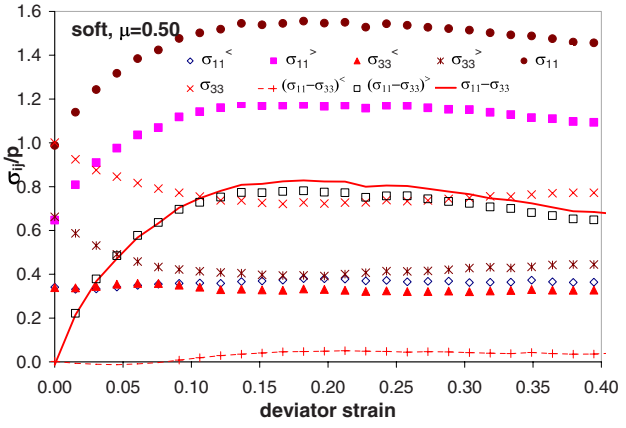

(b)

FIG. 6. (Color online) Contribution of strong and weak contacts to principal stresses and deviator stress (μ=0.50) in hard (a) and soft (b) granular assemblies under shearing.

shearing) [Figs. 4(a), 5(a), and 6(a)]. Incidentally, this contribution is also practically equal to the contribution of the strong contacts to the minor principal stress during postpeak regime for all values of friction in hard systems (i.e., $\sigma_{11}^{<}=\sigma_{33}^{<}=\sigma_{33}^{>}$ is satisfied in hard systems in the postpeak regime and practically independent of interparticle friction). However, in soft systems $\sigma_{11}^{<}=\sigma_{33}^{<}<\sigma_{33}^{>}$ throughout shearing [Figs. 4(b), 5(b), and 6(b)]. For a given value of interparticle friction, the contribution of the strong contacts to the major principal stress is practically constant and independent of the elastic modulus of particles during the postpeak regime (Figs. 4–6). For a given value of interparticle friction, the magnitude of the minor principal stress σ_{33} is higher in soft particle systems when compared with a hard system (Figs. 4–6). In soft systems, σ_{33} (and $\sigma_{33}^{>}$) decreases for increase in interparticle friction during shearing [Figs. 4(b), 5(b), and 6(b)]. We observe that, overall, the effect of elasticity of the particles has only a marginal influence on the magnitude of the major principal stress (and practically negligible influence during the postpeak period), but has a dominant effect on the magnitude of the minor principal stress component during shearing—decrease in elasticity of the particles strongly enhances the minor principal stress component of granular media during shearing. As a combined effect of the above roles, effectively the contribution of elasticity of particles to principal stress is unimodal and shear strength (deviator stress) increases with the elasticity of the particles in granular media.

Figure 7 shows that, irrespective of the elasticity of the particles, the peak and steady state values of shear stress ratio q/p increase with interparticle friction with a decreasing slope. Other recent studies for frictionless hard granular media (e.g., [21]) suggest that, though they do not dilate under shearing, they display macroscopic friction—thus suggesting that they can sustain shear strength. Although the shear-deformation behavior of frictionless granular media is somewhat outside the scope of the current study, we performed an additional simulation for the soft assembly when $\mu \to 0$ (0.01) and the results are incorporated in Fig. 7. From this we can confirm that, irrespective of the elasticity of the particles, frictionless three-dimensional granular media can sustain shear strength.

From the above discussions, we find that particle-scale friction and elasticity play significant roles in the micromechanical behavior of three-dimensional granular assemblies subjected to shearing. However, to understand their relative contributions when friction and elasticity act together in

TABLE I. Levels of contribution of particle-scale properties to quantities of stress tensor of the assemblies during shearing. The minor contributions account for less than about 7% for strong contacts and less than 3% for weak contacts.

	Increase in interparticle friction (μ)	Increase in particle-scale elasticity (E)
σ_{11} 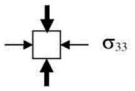 σ_{33}		
=		
$\sigma_{11}^{N>}$ ---->	Increases (major contribution)	Increases only up to peak state. Otherwise, mostly independent.
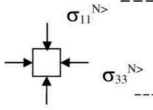 $\sigma_{33}^{N>}$ ---->	Decreases (major contribution)	Decreases (major contribution)
+		
$\sigma_{11}^{N<}$ ---->	Independent (minor contribution)	Increases (minor contribution)
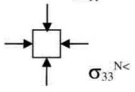 $\sigma_{33}^{N<}$ ---->	Independent (minor contribution)	Independent (minor contribution)
+		
$\sigma_{11}^{T>}$ ---->	Increases (minor contribution)	Decreases (minor contribution)
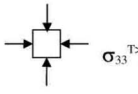 $\sigma_{33}^{T>}$ ---->	Decreases (minor contribution)	Decreases (minor contribution)
+		
$\sigma_{11}^{T<}$ ---->	Increases (minor contribution)	Decreases (minor contribution)
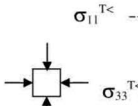 $\sigma_{33}^{T<}$ ---->	Decreases (minor contribution)	Decreases (minor contribution)

granular assemblies, we have also provided the following relative indices (RIs), viz., the RI of the stress ratio, the RI of the fabric anisotropy of strong contacts, and the RI of the sliding fraction (i.e., proportion of sliding contacts in relation

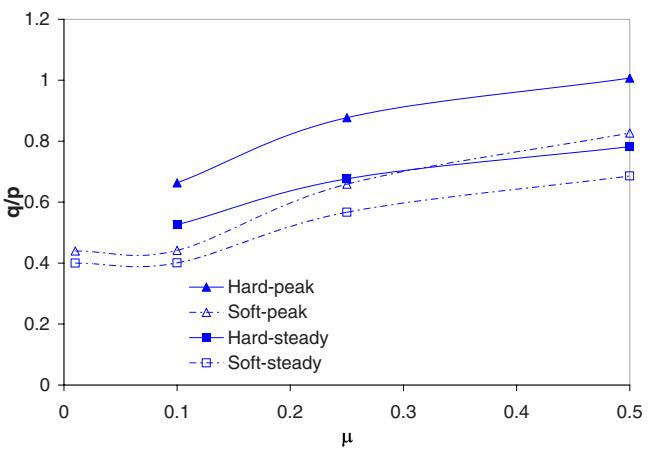

FIG. 7. (Color online) Shear stress ratio at peak and steady states.

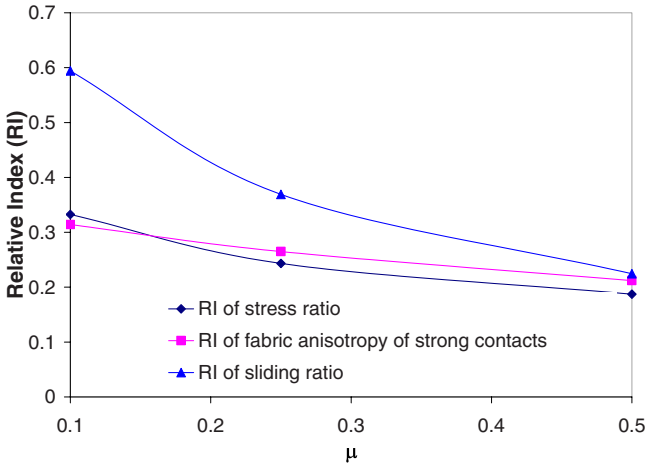

FIG. 8. (Color online) Measure of relative indices (RIs).

to total number of contacts at a given deviator strain level) plotted against the coefficient of interparticle friction. For a given value of interparticle friction, the RI of the (shear) stress ratio is the difference between the peak values of stress ratio q/p of hard and soft assemblies, normalized to that of the hard assembly. In the same way, the other indices were also calculated and presented in Fig. 8. We observe that the combined effects of elasticity of particles and interparticle friction are more pronounced in the relative indices of low-frictional granular systems. The indices of stress ratio and fabric anisotropy of strong contacts match more closely, as the shear strength in granular systems depends on the ability of the grains to sustain strongly anisotropic strong contacts [12,13].

B. Packing density, coordination number, and volumetric strain measures

The geometric stability of granular media under mechanical loading is commonly studied in terms of their apparent coordination number Z_a (i.e., average number of contacts per particle) at a given stage of loading. However, it is being recognised that the mechanical coordination number, Z_m (average number of load-bearing contacts per particle, so the coordination number computed when rattlers, i.e., particles without contacts or with just one contact, are excluded) is a better representation of geometric stability of a granular packing (e.g., [22]). Figure 9 shows the variation of packing density (packing fraction) and mechanical coordination number of the assemblies during shearing. Under constant mean stress condition, the packing density and mechanical coordination number of sheared granular assemblies increase for decreases in both interparticle friction and elasticity of particles. We point out that, in low-frictional granular systems, a relatively large number of contacts share the load and attain a higher value of packing density, although macroscopic shear strength decreases with decrease in interparticle friction. This is because, more than the packing density, it is the anisotropy of the strong load-bearing contacts that dictates shear strength in granular packing [12,13]. Furthermore, the packing density of the assemblies attains a constant value at

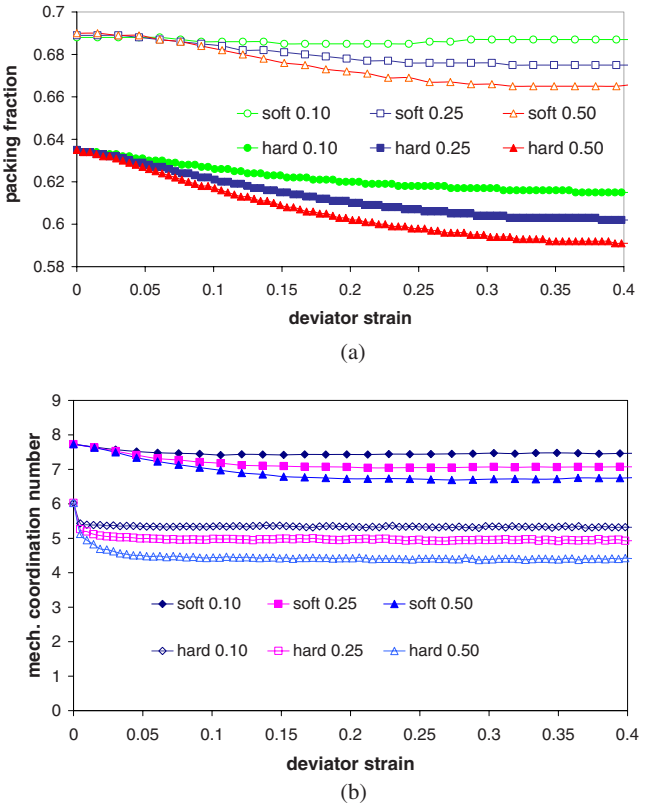

FIG. 9. (Color online) Variation of (a) packing density and (b) mechanical coordination number of the assemblies during shearing.

steady state (deviator strain about 0.35–0.4), as one would expect. However, we point out that it could be possible that if shearing continues further for "very large" deviator strain levels, the granular media could undergo "flow," resulting in a drop in their mechanical coordination number and packing density—further studies are required to examine the shear deformation behavior of granular media under very large deviator strain levels, which is outside the scope of the present study. Comparing Fig. 9 with Figs. 4–6, it is interesting to note that, at deviator strain levels corresponding to when systems attain peak shear strength, the mechanical coordination number attains a minimum value (critical mechanical coordination number) and thereafter remains constant during the postpeak shearing regime.

Figure 10 shows the variation of both apparent coordination number and mechanical coordination number in hard systems plotted against the deviatoric fabric of all and of strong contacts [10]. We observed that in the soft system the variations of both the apparent and mechanical coordination numbers were identical during shearing and hence plotted as single curves. In the hard system, the particles sustain a higher level of anisotropy of heavily loaded contacts with no significant drop in the measures of coordination numbers for most part of shearing (the variations present vertical lines soon after peak shear strength is initiated in the assemblies—the arrows indicate the progressive path of these measures with shearing). However, this is not the case for soft granular materials as a continuous change in mechanical coordination number occurs to sustain anisotropic strong forces during shearing. For a given value of interparticle friction, the geometric structures in hard systems (represented in terms of coordination numbers) sustain higher levels of fabric anisotropy of the strong contacts. During shearing, the soft system experiences a relatively less anisotropic distribution of forces as the forces are more evenly distributed across the available contacts, whereas the geometry of the hard system tends to develop a concentrated "rigid" sparse distribution of anisotropic forces across particle contacts. Figure 11 shows the variation of sliding fraction in the assemblies (i.e., the ratio of sliding contacts to the total number of contacts at a given deviator strain level). It is evident that the sliding fraction increases with elasticity of particles, more dominantly in low frictional systems. Generally, the variation of sliding presents "spiky" patterns in hard particulate systems and the spikes tend to smooth out for decrease in elasticity of particles (soft systems). Figure 12 shows the evolution of volumetric strain and the maximum dilation rate for the assemblies studied here. It is evident that both interparticle friction and elasticity of particles enhance the volumetric strain and the maximum

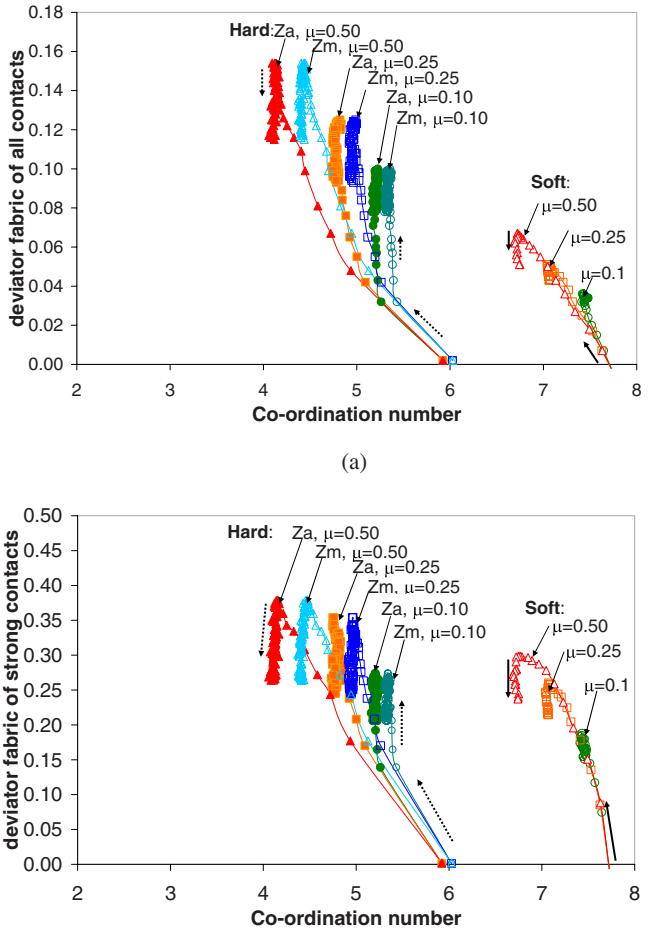

FIG. 10. (Color online) Variation of measures of fabric-coordination numbers during shearing. The plots show the variations of apparent coordination number (Z_a) and mechanical coordination number (Z_m) versus the deviator fabric of all the contacts (a) and the deviator fabric of strong contacts (b). In soft systems, the variation of Z_m and Z_a were almost identical and hence presented as single plots for different values of μ.

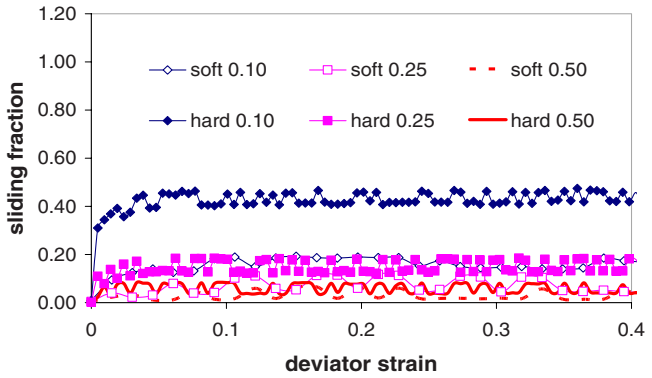

FIG. 11. (Color online) Variation of sliding fraction in the assemblies.

dilation rate. For the frictional assemblies used in this study, the maximum dilation rate varies linearly with the interparticle friction and its slope is practically independent of the elastic modulus of the particles. However, another recent study reports that frictionless rigid spheres ($\mu=0$) could have macroscopic friction, but no dilatancy [21]. Hence, we have extrapolated the lower end of the maximum dilation curve for hard assemblies as shown in dotted lines in Fig. 12. Further tests are required to precisely define the dilation behaviour of granular media having very low interparticle friction ($\mu<0.1$). However, we have performed an additional simulation here for the soft system with $\mu\rightarrow 0$ to determine its

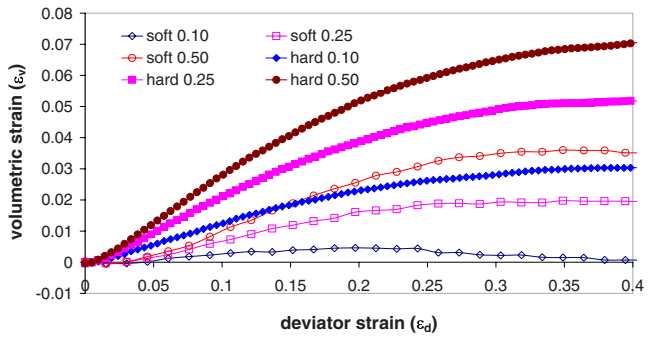

(a)

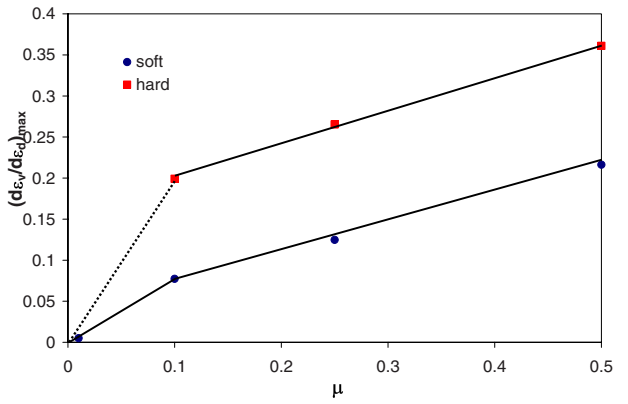

(b)

FIG. 12. (Color online) Variation of volumetric strain (a) and maximum dilation rate (b) during shearing.

dilation characteristics. We found that, indeed, elasticity of particles does not enhance the dilation behavior of frictionless granular systems. Other studies suggest that volumetric strains are mainly induced by tangential relative displacements corresponding to contact reorientations [23]. The volumetric strain increment of the strong network is postulated to be related to buckling-related reorientations of contacts in the strong network [2,24].

IV. CONCLUDING REMARKS

Information on the role of particle-scale properties on macroscopic shear strength (and other related measures of shear modulus and bulk friction) in granular media is investigated. From this analysis, we conclude that interparticle friction promotes the normal stress contribution of strong contacts to major principal stress σ_{11}, while it decreases the normal stress contribution of strong contacts to minor principal stress σ_{33} (bimodal contribution). As a net effect, friction promotes the deviator stress; thereby the shear strength of the granular assemblies increases with interparticle friction. We could speculate that, even in the limiting case of frictionless particulate systems, the anisotropy in the distribution of normal forces in the contacts and their subsequent contribution to principal stresses in sheared granular systems (mostly disordered) is just enough to establish a minimum level of macroscopic shear strength (or bulk friction) as observed in other studies (e.g., [21]). In other words, as previous studies have found a good level of correlation between the macroscopic shear strength and directional anisotropy of strong contacts [12,13], we suggest that the anisotropy that exists in the orientation of strong contacts (even in the case of initial isotropic packing under anisotropic loading, i.e., during shearing) could be responsible for the microscopic origin of shear strength in frictionless granular systems. The present study shows that apart from the early stages of shearing, particle-scale elasticity does not affect the contribution of strong contacts to the major principal stress, but decreases their contribution to the minor principal stress (unimodal contribution). Hence, friction promotes both major and minor principal stress components in sheared granular assemblies, whereas elasticity of particles mostly works through the minor principal stress during shearing. Although the modus operandi of friction and elasticity is different, both properties influence shear strength of granular media. Overall, interparticle friction "softens" the strong load-bearing contacts along the major principal stress direction, whereas both interparticle friction and particle-scale elasticity "stiffen" (reinforce) the strong load-bearing contacts that provide lateral stability along the minor principal stress direction. We have also shown here that the packing density is inversely related to interparticle friction and elasticity of particles. However, volumetric strain is proportional to both interparticle friction and elasticity of the particles. Interestingly, the maximum dilation rate in the assemblies varies linearly with interparticle friction and the slope is practically independent of elasticity of the particles when interparticle friction is more than about 0.1. We have observed that granular assemblies attain peak shear strength on attaining critical

mechanical coordination number during shearing. Thereafter, mechanical coordination number remains fairly constant during the postpeak regime, irrespective of the elasticity of particles. We also suggest that the elasticity of particles does not enhance dilation in frictionless granular media subjected to shearing. We expect that the insights provided here help to understand the role of particle-scale properties on the rather complex micromechanical behavior of granular media, in particular, shear strength under anisotropic loading conditions and to possibly understand their analogical counterpart of glass transition behavior [22,25].

ACKNOWLEDGMENT

We thank Elizabeth Awujoola for her support in this study.

[1] D. M. Mueth, H. M. Jaeger, and S. R. Nagel, Phys. Rev. E **57**, 3164 (1998).
[2] N. P. Kruyt and S. J. Antony, Phys. Rev. E **75**, 051308 (2007).
[3] M. R. Kuhn, Granular Matter **4**, 155 (2003).
[4] F. Radjai, S. Roux, and J. J. Moreau, Chaos **9**, 544 (1999).
[5] S. J. Antony and M. Ghadiri, J. Appl. Mech. **68**, 772 (2001).
[6] T. S. Majmudar, M. Sperl, S. Luding, and R. P. Behringer, Phys. Rev. Lett. **98**, 058001 (2007).
[7] B. Miller, C. O'Hern, and R. P. Behringer, Phys. Rev. Lett. **77**, 3110 (1996).
[8] A. Suiker and N. Fleck, J. Appl. Mech. **71**, 350 (2004).
[9] F. Radjai, M. Jean, J. J. Moreau, and S. Roux, Phys. Rev. Lett. **77**, 274 (1996).
[10] C. Thornton and S. J. Antony, Philos. Trans. R. Soc. London, Ser. A **356**, 2763 (1998).
[11] F. Radjai, in *Granular Materials: Fundamentals and Applications*, edited by S. J. Antony *et al.* (Royal Society of Chemistry, London, 2004), pp. 157–184.
[12] F. Radjai, e-print arXiv:0801.4722v1.
[13] S. J. Antony, Philos. Trans. R. Soc. London, Ser. A **365**, 2879 (2007).
[14] P. A. Cundall and O. D. L. Strack, Geotechnique **29**, 47 (1979).
[15] S. J. Antony, R. Moreno-Atanasio, J. M. Musadaidzwa, and R. A. Williams, J. Nanomater. **2008**, 125386 (2008).
[16] S. Ostojic, E. Somfai, and B. Nienhuis, Nature (London) **439**, 828 (2006).
[17] K. L. Johnson, *Contact Mechanics* (Cambridge University Press, Cambridge, U.K., 1985).
[18] R. D. Mindlin and H. Deresiewicz, J. Appl. Mech. **20**, 327 (1953).
[19] S. J. Antony and M. R. Kuhn, Int. J. Solids Struct. **41**, 5863 (2004).
[20] M. Satake, in *Deformation and Failure of Granular Materials*, edited by P. A. Vermeer and H. J. Luger (Balkema, Rotterdam, 1982), pp. 63–68.
[21] P. E. Peyneau and J. N. Roux, Phys. Rev. E **78**, 011307 (2008).
[22] F. Zamponi, Nature (London) **453**, 606 (2008).
[23] N. P. Kruyt and L. Rothenburg, Mech. Mater. **36**, 1157 (2004).
[24] F. Radjaï, D. E. Wolf, M. Jean, and J. J. Moreau, Phys. Rev. Lett. **80**, 61 (1998).
[25] A. J. Liu and S. R. Nagel, Nature (London) **396**, 21 (1998).